

## An insight on the mechanism of efficient leaching of vanadium from vanadium shale induced by microwave-generated hot spots

Sheng Li, Yimin Zhang, Yizhong Yuan, and Pengcheng Hu

Cite this article as:

Sheng Li, Yimin Zhang, Yizhong Yuan, and Pengcheng Hu, An insight on the mechanism of efficient leaching of vanadium from vanadium shale induced by microwave-generated hot spots, *Int. J. Miner. Metall. Mater.*, 30(2023), No. 2, pp. 293-302. <https://doi.org/10.1007/s12613-022-2459-7>

View the article online at [SpringerLink](#) or [IJMMM Webpage](#).

### Articles you may be interested in

Zhi-yuan Ma, Yong Liu, Ji-kui Zhou, Mu-dan Liu, and Zhen-zhen Liu, [Recovery of vanadium and molybdenum from spent petrochemical catalyst by microwave-assisted leaching](#), *Int. J. Miner. Metall. Mater.*, 26(2019), No. 1, pp. 33-40. <https://doi.org/10.1007/s12613-019-1707-y>

Subhmit K. Roy, Deepak Nayak, Nilima Dash, Nikhil Dhawan, and Swagat S. Rath, [Microwave-assisted reduction roasting–magnetic separation studies of two mineralogically different low-grade iron ores](#), *Int. J. Miner. Metall. Mater.*, 27(2020), No. 11, pp. 1449-1461. <https://doi.org/10.1007/s12613-020-1992-5>

Yun Guo, Hong-yi Li, Yi-heng Yuan, Jie Huang, Jiang Diao, Gang Li, and Bing Xie, [Microemulsion leaching of vanadium from sodium-roasted vanadium slag by fusion of leaching and extraction processes](#), *Int. J. Miner. Metall. Mater.*, 28(2021), No. 6, pp. 974-980. <https://doi.org/10.1007/s12613-020-2105-1>

Jing-peng Wang, Yi-min Zhang, Jing Huang, and Tao Liu, [Synergistic effect of microwave irradiation and  \$\text{CaF}\_2\$  on vanadium leaching](#), *Int. J. Miner. Metall. Mater.*, 24(2017), No. 2, pp. 156-163. <https://doi.org/10.1007/s12613-017-1390-9>

Yang He, Jian Liu, Jian-hua Liu, Chun-lin Chen, and Chang-lin Zhuang, [Carbothermal reduction characteristics of oxidized Mn ore through conventional heating and microwave heating](#), *Int. J. Miner. Metall. Mater.*, 28(2021), No. 2, pp. 221-230. <https://doi.org/10.1007/s12613-020-2037-9>

Jun-peng Wang, Tao Jiang, Ya-jing Liu, and Xiang-xin Xue, [Influence of microwave treatment on grinding and dissociation characteristics of vanadium titanomagnetite](#), *Int. J. Miner. Metall. Mater.*, 26(2019), No. 2, pp. 160-167. <https://doi.org/10.1007/s12613-019-1720-1>



IJMMM WeChat



QQ author group

# An insight on the mechanism of efficient leaching of vanadium from vanadium shale induced by microwave-generated hot spots

Sheng Li<sup>1,2,3,4)</sup>, Yimin Zhang<sup>1,2,3,4,5),✉</sup>, Yizhong Yuan<sup>1,2,3,4)</sup>, and Pengcheng Hu<sup>1,2,3,4)</sup>

1) School of Resource and Environmental Engineering, Wuhan University of Science and Technology, Wuhan 430081, China

2) State Environmental Protection Key Laboratory of Mineral Metallurgical Resources Utilization and Pollution Control, Wuhan University of Science and Technology, Wuhan 430081, China

3) Collaborative Innovation Center of Strategic Vanadium Resources Utilization, Wuhan 430081, China

4) Hubei Provincial Engineering Technology Research Center of High Efficient Cleaning Utilization for Shale Vanadium Resource, Wuhan University of Science and Technology, Wuhan 430081, China

5) School of Resource and Environmental Engineering, Wuhan University of Technology, Wuhan 430070, China

(Received: 16 November 2021; revised: 2 March 2022; accepted: 3 March 2022)

**Abstract:** Microwave heating can rapidly and uniformly raise the temperature and accelerate the reaction rate. In this paper, microwave heating was used to improve the acid leaching, and the mechanism was investigated via microscopic morphology analysis and numerical simulation by COMSOL Multiphysics software. The effects of the microwave power, leaching temperature,  $\text{CaF}_2$  dosage,  $\text{H}_2\text{SO}_4$  concentration, and leaching time on the vanadium recovery were investigated. A vanadium recovery of 80.66% is obtained at a microwave power of 550 W, leaching temperature of 95°C,  $\text{CaF}_2$  dosage of 5wt%,  $\text{H}_2\text{SO}_4$  concentration of 20vol%, and leaching time of 2.5 h. Compared with conventional leaching technology, the vanadium recovery increases by 6.18%, and the leaching time shortens by 79.17%. More obvious pulverization of shale particles and delamination of mica minerals happen in the microwave-assisted leaching process. Numerical simulation results show that the temperature of vanadium shales increases with an increase in electric field (E-field). The distributions of E-field and temperature among vanadium shale particles are relatively uniform, except for the higher content at the contact position of the particles. The analysis results of scale-up experiments and leaching experiments indicate high-temperature hot spots in the process of microwave-assisted leaching, and the local high temperature destroys the mineral structure and accelerates the reaction rate.

**Keywords:** vanadium shale; microwave-assisted leaching; hot spots; numerical simulation

## 1. Introduction

Vanadium shale is an important vanadium resource in China, with abundant reserves and wide distribution [1–2]. Extracting vanadium from shale is of great significance to the development and utilization of vanadium resources in China [3–4]. The grade of vanadium pentoxide ( $\text{V}_2\text{O}_5$ ) in shale is usually in the range of 0.3wt%–1.3wt%, belonging to low-grade vanadium resources [5–6]. Most vanadium exists in the form of vanadium(III) and is stable in the lattice structure of aluminosilicates by isomorphism instead of Al(III), making its extraction difficult [7–8]. Compared with the roasting acid leaching process, direct acid leaching simultaneously completes ore decomposition and vanadium's extraction in the acid leaching process, significantly shortening the process flow [9–10]. In addition, the acid leaching process also complies with the “dual carbon goals” (carbon peak and carbon neutrality) policy proposed by China, one of the reasons why the direct acid leaching process has become the focus of attention in recent years.

Direct acid leaching of vanadium is a clean and low energy consumption process. A certain concentration of sulfuric acid directly destroys the mineral structure of vanadium shale and lets  $\text{H}^+$  enter the lattice, releasing vanadium from aluminosilicate minerals, such as mica and illite [11]. The structure of vanadium-bearing aluminosilicate is stable, so it takes sulfuric acid a long time to react to destroy its structure. Moreover, with recent progress in the leaching process, the gray matter layer on the mineral surface thickens, which affects the mass transfer of  $\text{H}^+$  and reduces the reaction rate [12]. Therefore, the problems of large acid consumption and long leaching time in the direct leaching process seriously hinder the development of the process.

Microwave irradiation is an effective and eco-friendly heating technology widely used in the mining field, especially metal extraction [13–16]. Wen *et al.* [17] reported that the interface reaction temperature and surface energy increased under microwave heating, which increased the reaction temperature, leaching recovery of copper, and reduced leaching time. Zhang *et al.* [18] studied the leaching process

✉ Corresponding author: Yimin Zhang E-mail: [zym126135@126.com](mailto:zym126135@126.com)

© University of Science and Technology Beijing 2023

of zinc from indium zinc ferrite (IBZF) by microwave heating. The result showed that microwave intensified the leaching reaction of IBZF. Microwaves had a significant nonthermal effect on the leaching reaction. The effective collision and the  $\text{H}_2\text{SO}_4$  activation under microwaves were attributed to the nonthermal microwave effect. For vanadium extraction from shale, Wang *et al.* [19–20] found that microwaves promoted the ion orientation movement and increased the diffusion rate of  $\text{H}^+$  and  $\text{F}^-$  towards solid–liquid reaction interface, and achieved a molecular level stirring. Therefore, microwaves have a broad prospect in vanadium leaching from shale. However, there is no systematic research process, and the enhanced mechanism based on microwave electromagnetic properties is still under debate.

Different views have been suggested for the enhanced mechanism [21–22]. Some researchers thought microwave-induced internal stress between different minerals reduced particle size and made the surface more porous [23–25]. To some extent, an increased surface area and porosity enhanced the mass transfer effect of leaching. However, it is not sufficient because reducing the particle size of shale via fine grinding could not achieve the same effect. Furthermore, some researchers suggested that microwaves directly act on mica lattice, making the decomposition in a microwave field [26–27]. This view is also unreasonable because the microwave absorption characteristics of mica are inferior, and microwaves do not affect it.

In the field of microwave high-temperature treatment of solid inorganic powder, the electric field intensification is proposed to explain that microwave sintering can significantly accelerate the sintering shrinkage [28–29]. The results showed that the electric field (E-field) intensity reached the maximum near the contact between particles. The maximum E-field intensity was much higher than the applied E-field intensity. At the same time, when the material exhibited a high dielectric loss, the E-field was intensified, showing extremely high heating rates and high-temperature hot spots [30–31]. These hot spots usually appear instantaneously at small particles’ contact interfaces, so their measurement is often difficult. Therefore, it is difficult to accurately detect the actual temperature of hot spots in the microwave leaching process in the laboratory. In this work, the E-field intensification and hot spots in the microwave leaching process

were analyzed by the simulation method. The E-field intensification and its associated hot spots are vital for enhancing vanadium extraction from shale by microwave.

In this paper, the effects of microwave power, leaching temperature,  $\text{CaF}_2$  dosage,  $\text{H}_2\text{SO}_4$  concentration, and leaching time on vanadium recovery were investigated. The conventional experiments were carried out as a control. Based on essential characteristics of electromagnetic heating in the microwave field, simulations and extended experiments were combined to explain the enhanced mechanism of microwave heating. This study provides a new idea to study the mechanism of efficient leaching of vanadium from vanadium shale by microwave heating.

2. Experimental

2.1. Materials

Vanadium shale used in the study was obtained from Pengze County, Jiangxi Province, China. The raw sample was ground to  $-0.074\text{ mm}$ , occupying for about 70wt%. The reagents used in this study were analytically pure. The chemical composition analysis of raw ore is shown in Table 1, and X-ray diffraction (XRD) and microscopic observation and elemental (SEM–EDS) images are shown in Fig. 1. The grade of  $\text{V}_2\text{O}_5$  in the raw sample was 0.88%. Fig. 1 shows the correlation of V, O, Al, Si, and K. The atomic composition of V, O, Al, Si, and K was similar to muscovite, indicating the presence of vanadium in muscovite. The valence distribution of vanadium in raw ore was determined by potentiometric titration [4], and the results are shown in Table 2. Among them, V(III) accounted for 72.15wt%, V(IV) accounted for 27.85wt%, but V(V) was not observed. Therefore, the vanadium shale used in this study belonged to the typical mica type vanadium shale.

2.2. Procedures

Mas-II plus microwave reactor was used in this study (SINEO Microwave Chemistry Technology Co., Ltd., China)

Table 1. Main chemical composition of the vanadium shale wt%

$\text{V}_2\text{O}_5$	$\text{SiO}_2$	$\text{Al}_2\text{O}_3$	$\text{Fe}_2\text{O}_3$	$\text{MgO}$	$\text{K}_2\text{O}$	$\text{CaO}$	$\text{Na}_2\text{O}$	P
0.88	64.84	9.86	4.74	1.57	2.44	3.74	2.04	0.40

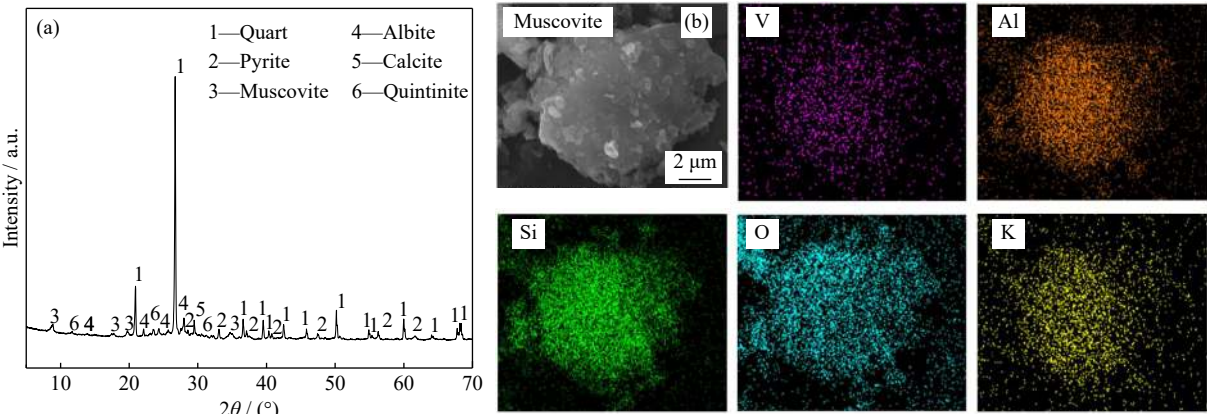


Fig. 1. (a) XRD pattern and (b) SEM–EDS analyses of the raw sample.

Table 2. Valence distribution of vanadium in raw ore %		
V(III)	V(IV)	V(V)
72.15	27.85	0

for microwave heating. 50 g raw sample was put in a 250 mL grinding flask with a certain mass ratio of CaF<sub>2</sub> and mixed with sulfuric acid in a solid/liquid ratio of 1:1.5 g/mL. The flask was heated in the microwave oven, and the solution was stirred with a digital magnetic stirrer. After leaching, the pulp was filtered, and the leaching recovery of V was calculated by the following formula:

$$R = \frac{C \times V}{\alpha \times m} \times 100\%$$

(1)

where *R* is the vanadium recovery; *C* is the vanadium concentration in leachate, g/L; *V* is the volume of the leachate, L; *α* is the vanadium grade of the raw sample; *m* is the mass of the raw sample, g.

The conventional leaching experiments were performed in a water bath under traditional electric heating, and other leaching conditions were consistent with microwave-assisted leaching.

2.3. Analytical methods

X-ray diffraction (XRD) analyses of shale samples were conducted using an Empyrean X-ray diffractometer (PANalytical Company, Netherlands). The test conditions were as follows: Cu K<sub>α</sub>, scanning speed of 15°/min, scanning range of 5°–90°, tube voltage of 40 kV, and tube current of 40 mA. Microscopic observation and elemental analysis (SEM–EDS) were performed using a JEOL JSM-6610 scanning electron microscope (JEOL, Japan) equipped with a Bruker QUANTAX200-30 energy dispersive spectrometer (Bruker, Germany). COMSOL Multiphysics software (COMSOL Inc., Sweden) was used for numerical simulation. The particle size distribution of the leaching residues was analyzed by a laser particle size analyzer (BT-9300H, Dandong Bettersize Instrument Co., Ltd., China)

3. Results and discussion

3.1. Comparison of microwave-assisted leaching and conventional leaching methods

3.1.1. Effect of the microwave power on the vanadium recovery

The effect of the microwave power (250–750 W) on the vanadium recovery was investigated at a leaching temperature of 95°C, CaF<sub>2</sub> dosage of 5wt%, H<sub>2</sub>SO<sub>4</sub> concentration of 20vol%, and leaching time of 2.5 h, and the results are shown in Fig. 2. With the increase in microwave power, an obvious increase in vanadium recovery is observed. When the microwave power exceeds 550 W, the vanadium recovery remains stable at 80.66%. Thus, 550 W is selected as the appropriate microwave power in the following experiments. With an increase in microwave power, the power density per unit volume of leaching solution also increases, promoting the migration and mass transfer of ions.

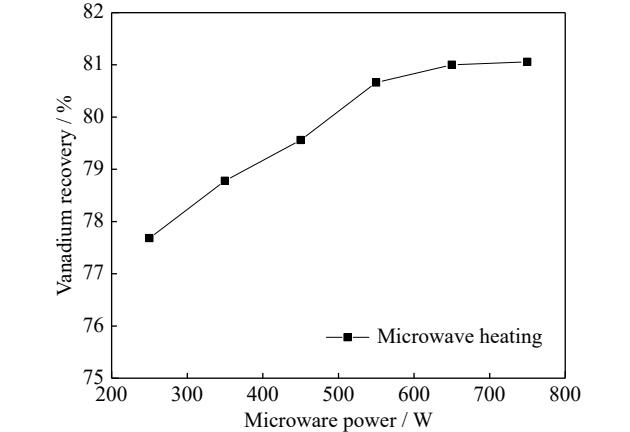


Fig. 2. Effects of the microwave power on the vanadium recovery.

3.1.2. Effect of the leaching temperature on the vanadium recovery

Under optimized conditions, the effect of the leaching temperature (55–95°C) on the vanadium recovery was investigated, and the results are shown in Fig. 3. The leaching temperature shows a significant effect on the vanadium recovery. With the temperature rising from 55 to 95°C, the vanadium recovery increases by 30%–40%. At the same leaching temperature, the leaching recovery of vanadium by microwave heating is higher than that by conventional heating, and the difference is up to 20%. In two leaching systems, due to the increase in temperature, the activity of reactants increases, the diffusion rate of H<sup>+</sup> and the dissolution rate of vanadium accelerate, leading to an increase in vanadium recovery [32]. When the leaching temperature exceeds 95°C, the evaporation rate of water and the equipment loss increase, reducing the leaching recovery. Therefore, the leaching temperature of 95°C (microwave power 550 W) is selected for the following experiments.

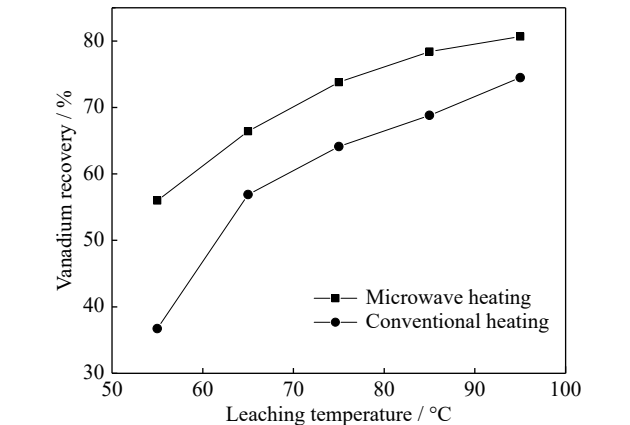


Fig. 3. Effect of the leaching temperature on the vanadium recovery.

3.1.3. Effect of the CaF<sub>2</sub> dosage on the vanadium recovery

Then the effects of the CaF<sub>2</sub> dosage (2wt%–6wt%) on the vanadium recovery were investigated, and the results are shown in Fig. 4. In both leaching methods, the vanadium recovery shows a trend of first increasing and then decreasing with the increase in CaF<sub>2</sub> dosage. When the dosage of CaF<sub>2</sub> is



5wt%, the vanadium recovery reaches the highest value.  $\text{CaF}_2$ , as a leaching additive, significantly promotes the leaching of vanadium from shale. However, when  $\text{CaF}_2$  is in excess, calcium ions combine with sulfate ion in sulfuric acid to form calcium sulfate. This is mainly because as the  $\text{CaSO}_4$  protective layer becomes thicker, the diffusion of sulfate and vanadate ions through the product layer becomes more difficult [33–35]. Comparing the two leaching methods, microwave-assisted leaching effectively enhances the leaching effect of  $\text{CaF}_2$ . It shows that microwave field and  $\text{CaF}_2$  have a synergistic impact on the system, which is also consistent with the research conclusion of relevant literatures [36–37].

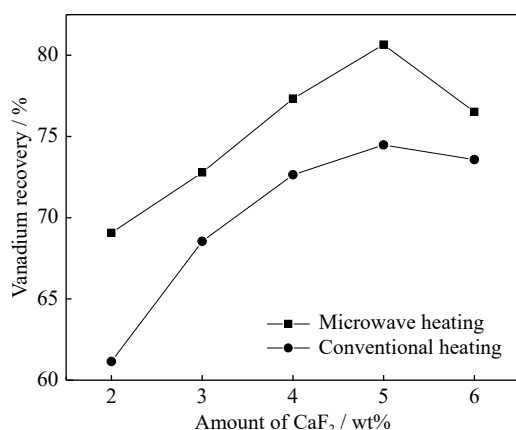


Fig. 4. Effect of  $\text{CaF}_2$  addition on the vanadium recovery.

### 3.1.4. Effect of $\text{H}_2\text{SO}_4$ concentration on the vanadium recovery

The effect of different  $\text{H}_2\text{SO}_4$  concentrations (5vol%–25vol%) on the vanadium recovery was investigated at a microwave power of 550 W, leaching temperature of  $95^\circ\text{C}$ , a  $\text{CaF}_2$  dosage of 5wt%, and leaching time of 2.5 h, and results are shown in Fig. 5. The vanadium recovery increases with the increase in  $\text{H}_2\text{SO}_4$  concentration, and when the  $\text{H}_2\text{SO}_4$  concentration reaches 20vol%, the growth trend of the vanadium recovery decreases. Although higher concentration of sulfuric acid will destroy vanadium mica, it will introduce excessive sulfate ions. Sulfate ions combine with calcium ions in calcium fluoride to form calcium sulfate, which af-

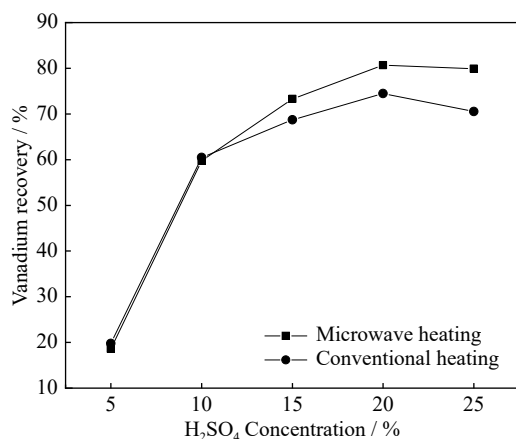


Fig. 5. Effect of the  $\text{H}_2\text{SO}_4$  concentration on the vanadium recovery.

fects the mass transfer process and reduces the leaching recovery of vanadium. In both leaching methods, the leaching recoveries of vanadium are almost the same when the concentration of  $\text{H}_2\text{SO}_4$  is lower than 10vol%. When the concentration exceeds 10vol%, the microwave-assisted leaching method shows the advantages in vanadium recovery. Within the scope of this experiment, the maximum difference in vanadium recovery is 10% at 25vol%  $\text{H}_2\text{SO}_4$  concentration. However, a further high concentration of  $\text{H}_2\text{SO}_4$  leads to more impurity ions entering the leaching solution and increases the alkali consumption in the subsequent process. Thus, 20vol% is selected as a suitable  $\text{H}_2\text{SO}_4$  concentration with a 6% gap of vanadium recovery between microwave-assisted leaching and conventional leaching method.

### 3.1.5. Effect of the leaching time on the vanadium recovery

The effect of the leaching time on the vanadium recovery was also investigated under optimized conditions, and the results are shown in Fig. 6. After a rapid rise, a gradually stabilized trend appears in both leaching methods with two obvious differences. Firstly, the growth rate of vanadium recovery in microwave-assisted leaching is significantly higher than that in conventional leaching. The vanadium recovery remains stable after 2.5 h of leaching. However, the steady point of vanadium recovery in conventional leaching is around 5 h, and there is still a slow growth when it exceeds 5 h. Secondly, when the leaching time reaches 2.5 h in microwave-assisted leaching, the vanadium recovery exceeds 80%, whereas in conventional leaching, the vanadium recovery of 80% appears after 12 h. For 80% vanadium recovery, the leaching time of microwave-assisted leaching is shortened by 79.17% compared with the conventional leaching. The improvement in vanadium recovery by microwave heating is significant.

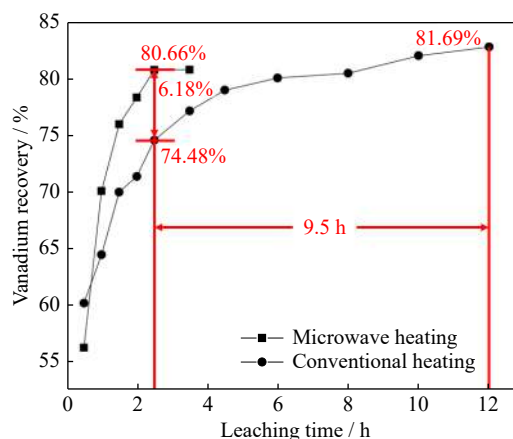
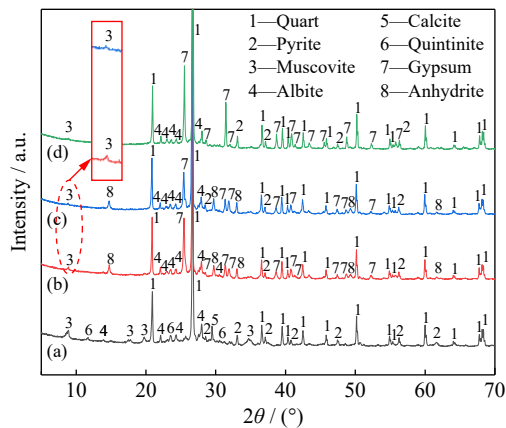


Fig. 6. Effect of leaching time on the vanadium recovery.

## 3.2. Comparisons of mineral transformation and micro-morphology of leaching residues

The XRD analyses of leaching residues under optimized conditions in microwave-assisted leaching were conducted to compare the mineral transformations in different leaching processes (Fig. 7). The results indicate that the diffraction peak of muscovite after leaching is weakened. The diffrac-

tion peak of muscovite is the lowest in Fig. 7(c), indicating the destruction of the muscovite structure by microwave-assisted leaching is more severe. At the same time, the diffraction peaks of muscovite in (c) and (d) are almost the same, indicating that microwave-assisted leaching for 2.5 h and conventional leaching for 12 h have the same leaching effect.



**Fig. 7.** XRD patterns of minerals: (a) raw ore; (b) leaching residues after 2.5 h of conventional leaching; (c) leaching residues after 2.5 h of microwave-assisted leaching; (d) leaching residues after 12 h of conventional leaching.

To intuitively compare the influence of two heating methods on leaching, the raw ore and leaching residues are analyzed by SEM–EDS, and the results are shown in Fig. 8. The particle size distribution of the leaching residues obtained after microwave heating and conventional heating is shown in Fig. 9. From the SEM images and particle size distribution,

it can be seen that the micromorphology of leaching residues is quite different under the same leaching conditions and different heating methods. Compared with the particle size of leaching residues, it is obvious that the particle size obtained by microwave-assisted leaching is smaller. At the same time, through the comparison of muscovite A, B, and C in Fig. 8, it can be seen that the mica minerals in the leaching residues have a dissolution erosion phenomenon. However, the lamellar structure of mica minerals after microwave-assisted leaching is exfoliated, and the dissolution erosion phenomenon is more severe. Compared with conventional leaching, the layered exfoliation structure of vanadium-bearing mica in leaching residues after microwave-assisted leaching is more conducive to the release of vanadium.

XRD and SEM–EDS analyses show that microwave heating can refine the mineral particle size, promoting the active surface of vanadium shale particles exposed to the reaction solution and accelerating the diffusion efficiency. At the same time, the lamellar structure of mica minerals after microwave-assisted leaching is exfoliated, which is conducive to the release of vanadium. Therefore, the application of microwave heating in the leaching process is beneficial to improving the release of vanadium from vanadium-bearing mica and shortening the leaching time.

3.3. Electromagnetic–thermal multi-physics simulation

3.3.1. Numerical model

Microwaves are fundamentally a kind of electromagnetic wave with a designated frequency range. The study of the enhanced mechanism of microwave-assisted leaching of vana-

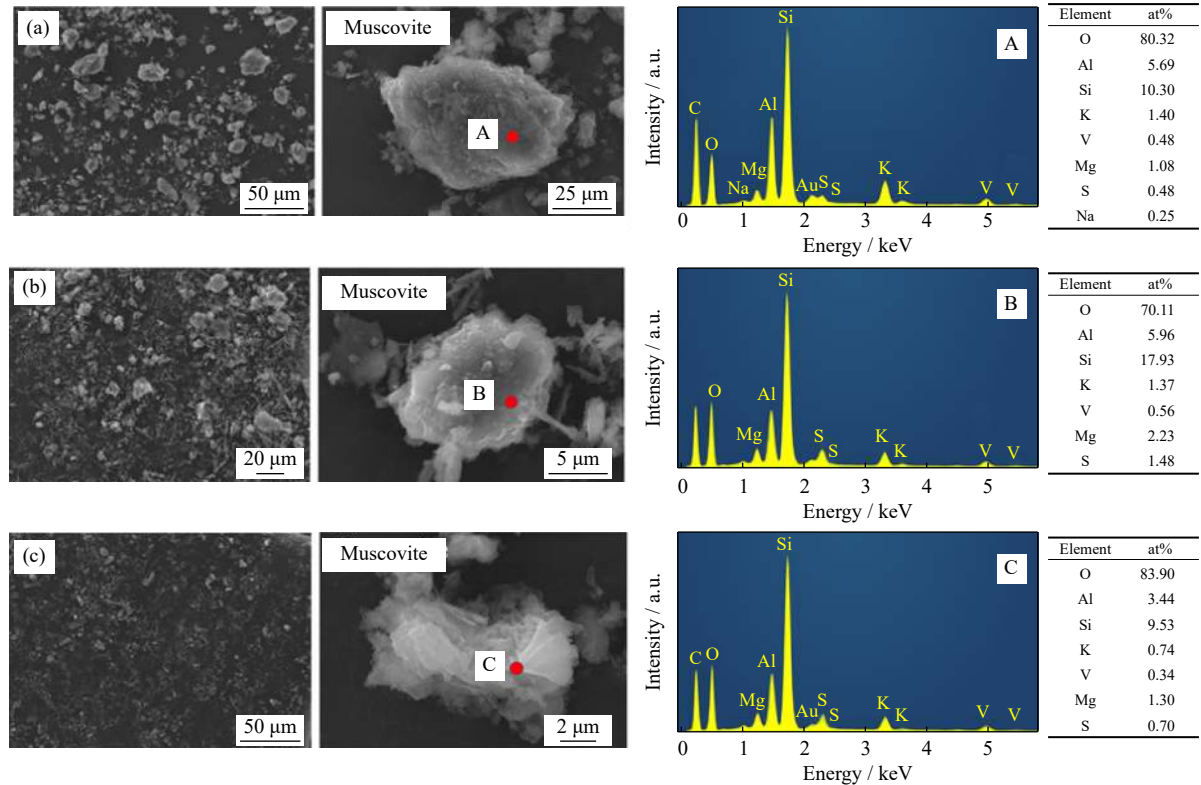


**Fig. 8.** SEM images and EDS element mapping of minerals: (a) raw ore; (b) leaching residues after 2.5 h of conventional leaching; (c) leaching residues after 2.5 h of microwave-assisted leaching.

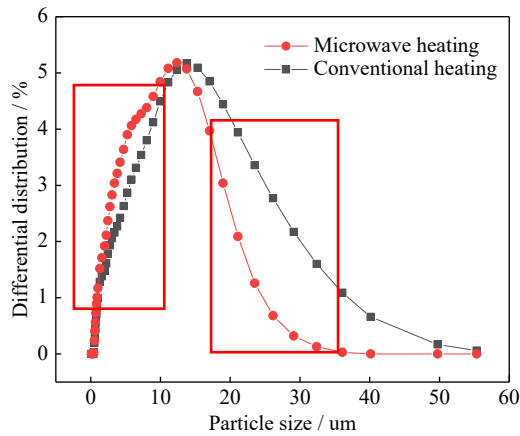


Fig. 9. Particle size distribution of the leaching residues.

dium is based on their electromagnetic properties. As the introduction states, the enhancement in E-field and its related hot spots may be the key to improve vanadium extraction from shale by microwave. Using the electromagnetic heating module in COMSOL software, the distributions of E-field intensity and temperature of different particle conditions in microwave-assisted leaching are simulated. The model is designed according to the size of the microwave oven used in the laboratory. The geometry of the microwave-assisted leaching model is shown in Fig. 10.

The geometric dimensions of the microwave cavity, waveguide, leaching environment, and vanadium shale

particle are shown in Table 3. The atmosphere inside the cavity is air, the relative permittivity of air is 1.0, the material of the cavity is made of brass with a relative permittivity of 1.0, the relative permittivity of the vanadium shale is 15.433-j4.351, and the relative permittivity of the water ball model is 80-j8. The microwave E-field and temperature field are simulated by using the microwave heating module and solid heat transfer module in COMSOL simulation software. The frequency of the incident wave is 2.45 GHz and the power is 550 W. The excitation for the microwave oven occurs through a rectangular waveguide installed on the left side of the cavity. The dominant mode of the transverse electric wave is TE<sub>10</sub> mode.

3.3.2. E-field and temperature distributions of vanadium shale in air

In this part, a series of simulations are conducted to evaluate the effects of microwave on E-field and temperature distributions of shale vanadium under different environments. To simplify the model, water replaces the acid solution in the simulation. Fig. 11(a)–(c) shows the E-field and temperature distributions between vanadium shale particles in the air. Fig. 11(d)–(f) shows E-field and temperature distributions between vanadium shale particles and water droplets in the air.

The distributions of E-field and temperature among particles are relatively uniform, except at the contact position of particles. Under microwave irradiation, the maximum E-field between vanadium shale particles in Fig. 11(a) reaches

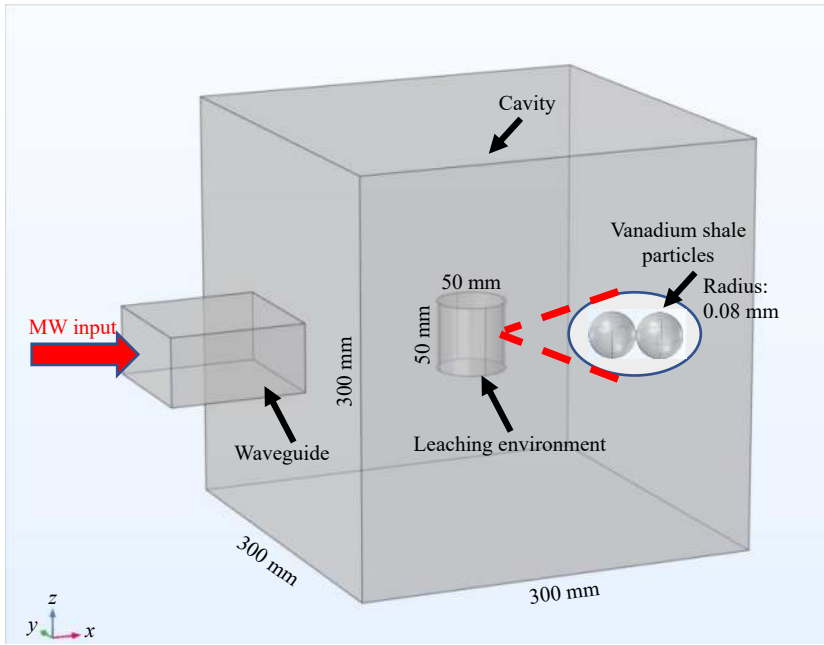
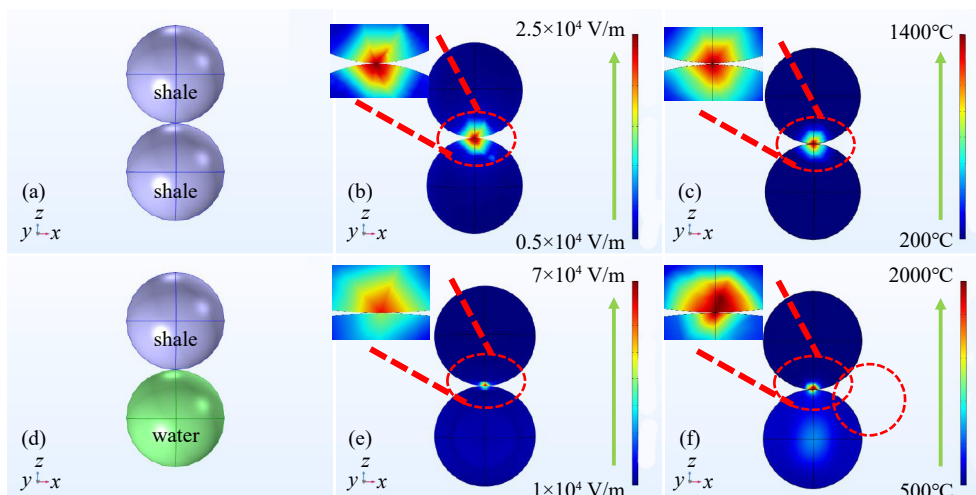


Fig. 10. Three-dimensional geometry of microwave-assisted leaching model.

Table 3. Basic parameters of the three-dimensional geometric model

Item	High / mm	Length / mm	Width / mm	Radius / mm
Microwave cavity	300	300	300	
Waveguide	50	100	100	
Leaching environment	50			25
Vanadium shale particle				0.08



**Fig. 11.** Simulation of E-field and temperature distributions on (a–c) particle–particle in air and (d–f) particle–water in air: (a, d) three-dimensional model of shales and water; (b, e) simulation of E-field distribution; (c, f) simulation of temperature distribution.

$2.5 \times 10^4$  V/m, and the maximum temperature reaches  $1400^\circ\text{C}$ . In the same case, the maximum E-field between vanadium shale particle and water droplet in Fig. 11(d) reaches  $7 \times 10^4$  V/m and the maximum temperature reaches  $2000^\circ\text{C}$ . The relative permittivity is used to express the ability of a material to absorb electromagnetic energy. Because the permittivity of water is greater than that of vanadium shale, the E-field intensity of particles in Fig. 11(a) is much higher than that of particles in Fig. 11(d). The E-field emission intensity determines the heat loss from electromagnetic energy and an increasing E-field intensity results in faster temperature rise under microwave irradiation [38–39].

To verify the reliability of the simulation, an extended experiment was carried out on vanadium shale with particle size of 2–3 cm. Two vanadium shales were put in a microwave reactor (frequency 2.45 GHz, input power 550 W). After starting the microwave oven, it was found that two vanadium shales in an extremely short time (1–3 s) cause severe ignition at the contact point (as shown in Fig. 12(a)–(d));

however, this phenomenon is not observed in the untouched part. Fig. 12(e) shows an SEM image of the contact part, indicating the damaged mineral structure of this part. As shown in Fig. 12(f)–(h), there are a large number of holes, cracks, and even molten materials, indicating that the generated temperature is extremely high. The experimental results show that there are high-temperature hot spots at the contact part of vanadium shale particles under microwave irradiation, which is consistent with the simulation results.

### 3.3.3. E-field and temperature distributions of vanadium shale in water

Fig. 13 shows the E-field and temperature distributions between vanadium shale particles in water. As shown in Fig. 13(a)–(c), the E-field intensity also increases as the number of vanadium shales increases. In a single vanadium shale, the maximum E-field intensity is in the middle, and the minimum is at both ends. When multiple particles gather, the maximum E-field intensity is observed at the contact position of particles, consistent with the simulation results. As shown in

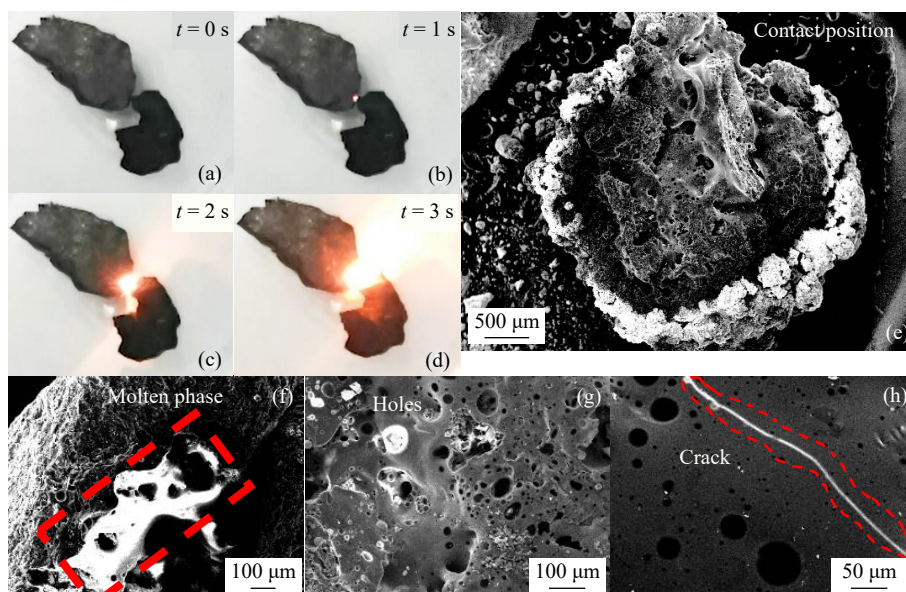


**Fig. 12.** (a–d) Hot spots generation process in air; (e–h) SEM images of minerals at the contact point.



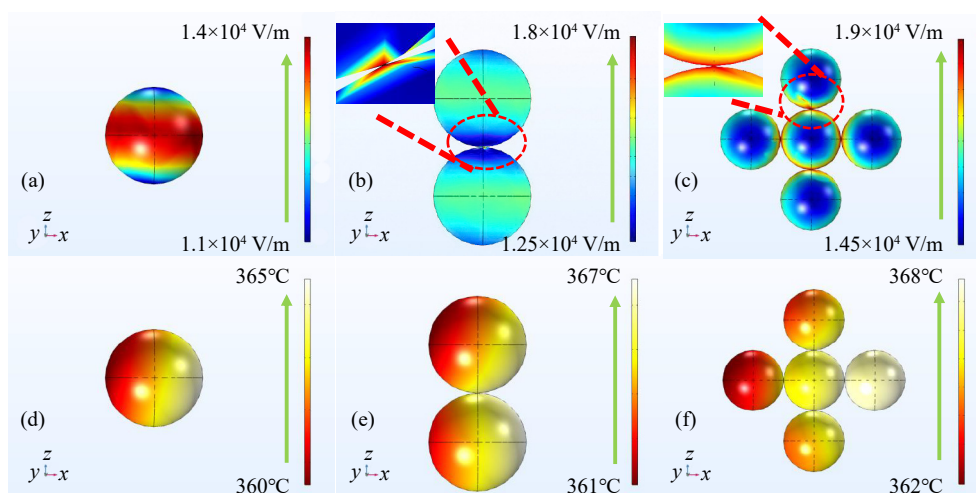


Fig. 13. Simulations of (a–c) E-field distribution and (d–f) temperature distribution on particles in water with an increase in the number of vanadium shales.

Fig. 13(d)–(f), with an increase in the number of vanadium shales, the temperature slightly increases, and the maximum temperature is observed at the contact position of particles.

Furthermore, the surface temperature of the solution environment is recorded every 10 s during microwave heating (Fig. 14). Experimental results suggest that the surface temperature distribution of the solution environment recorded by the laboratory experiment agrees closely with the simulation results in our model.

Compared with Fig. 11, the E-field intensity and temperature in Fig. 13 decrease significantly and simultaneously. Combined with Fig. 15, the results show that the temperature generated between particles is still higher than that of the solution environment. Furthermore, an extended experiment is carried out to verify the simulation results. Two vanadium shales with a particle size of 2–3 cm are put in water and heated under the microwave (frequency of 2.45 GHz, input power of 550 W). In Fig. 16(a)–(d), the ignition phenomenon on happening in Fig. 12(b)–(c) is not captured. However, the water near the vanadium shales begins to boil first.

This phenomenon is in good agreement with the simulation results of Figs. 14 and 15. Comparing Fig. 16(g) and Fig. 16(e), (f), and (h), it can be seen that after microwave

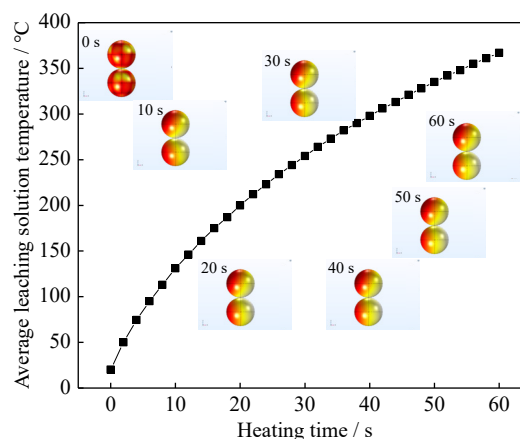


Fig. 15. Effect of microwave heating time on the average temperature of vanadium shale.

heating, the mineral surface and structure at the contact are damaged, accompanied by mineral detritus and cracks. This is also consistent with the change in mica structure in Fig. 8(b) and (c), indicating that the high-temperature hot spots generated during microwave heating damage the mica structure to a certain extent, thereby accelerating the reaction rate.

## 4. Conclusion

Leaching vanadium shale by microwave heating can greatly shorten the leaching time. Compared with conventional leaching, microwave-assisted leaching increases the leaching recovery of vanadium by 6.18% and shortens the leaching time by 79.17%. The E-field intensity and temperature in vanadium shale particles decrease with the increase of the permittivity in the medium; the maximum E-field intensity and temperature always exist at the contact position between vanadium shale particles. In addition, with the increase in vanadium shale particle aggregation, the E-field intensity and temperature increase in different ranges. In microwave heating leaching, with the input of microwave, the E-field intensity and temperature in vanadium shale particles increase, and high-temperature hot spots are formed on the

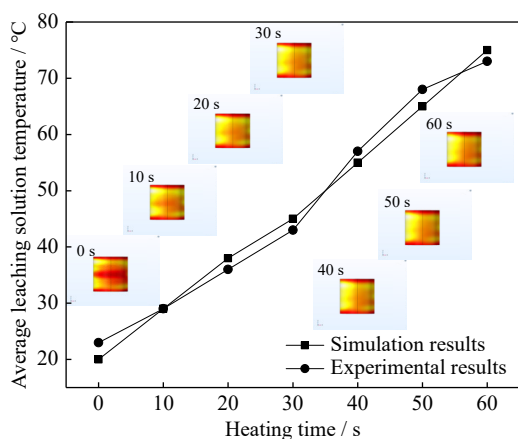
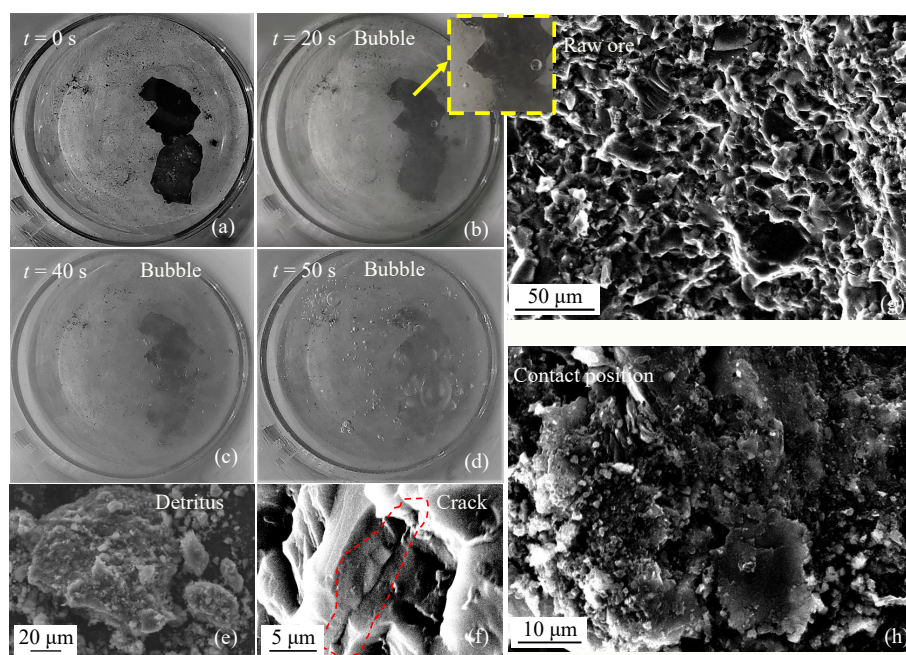


Fig. 14. Temperature validation of water under microwave heating.



**Fig. 16.** (a–d) Hot spots generation process in water; (e) SEM image of mineral detritus at the contact point; (f) SEM image of crack on mineral at the contact point; (g) SEM image of raw ore; (h) SEM image of minerals at the contact point.

surface of vanadium shale particles. This temperature destroys the mineral structure, refines the particle size of minerals, and peels off the layered structure of mica. With the increase in the exposed surface of vanadium-bearing minerals, the collision frequency between hydrogen ions and active sites increases, the reaction rate increases, and the leaching time shortens.

## Acknowledgements

This study was financially supported by the National Natural Science Foundation of China (No. 51904211) and the National Natural Science Foundation of China (No. 52004187).

## Conflict of Interest

The authors declare that they have no known competing financial interests or personal relationships that could have appeared to influence the work reported in this paper.

## References

- [1] Y.M. Zhang, S.X. Bao, T. Liu, T.J. Chen, and J. Huang, The technology of extracting vanadium from stone coal in China: History, current status and future prospects, *Hydrometallurgy*, 109(2011), No. 1-2, p. 116.
- [2] J.P. Gustafsson, Vanadium geochemistry in the biogeosphere-speciation, solid-solution interactions, and ecotoxicity, *Appl. Geochem.*, 102(2019), p. 1.
- [3] E. del Carpio, L. Hernández, C. Ciangherotti, et al., Vanadium: History, chemistry, interactions with  $\alpha$ -amino acids and potential therapeutic applications, *Coord. Chem. Rev.*, 372(2018), p. 117.
- [4] P.C. Hu, Y.M. Zhang, T. Liu, J. Huang, Y.Z. Yuan, and Q.S. Zheng, Highly selective separation of vanadium over iron from stone coal by oxalic acid leaching, *J. Ind. Eng. Chem.*, 45(2017), p. 241.
- [5] B. Chen, S.X. Bao, Y.M. Zhang, and S. Li, A high-efficiency and sustainable leaching process of vanadium from shale in sulfuric acid systems enhanced by ultrasound, *Sep. Purif. Technol.*, 240(2020), art. No. 116624.
- [6] Y.Z. Yuan, Y.M. Zhang, T. Liu, P.C. Hu, and Q.S. Zheng, Optimization of microwave roasting-acid leaching process for vanadium extraction from shale via response surface methodology, *J. Cleaner. Prod.*, 234(2019), p. 494.
- [7] Y.Z. Yuan, Y.M. Zhang, T. Liu, T.J. Chen, and J. Huang, Source separation of V and Fe by two-stage selective leaching during V extraction from stone coal, *RSC Adv.*, 7(2017), No. 30, p. 18438.
- [8] B. Chen, S.X. Bao, and Y.M. Zhang, Synergetic strengthening mechanism of ultrasound combined with calcium fluoride towards vanadium extraction from low-grade vanadium-bearing shale, *Int. J. Min. Sci. Technol.*, 31(2021), No. 6, p. 1095.
- [9] M.T. Li, C. Wei, G. Fan, H.L. Wu, C.X. Li, and X.B. Li, Acid leaching of black shale for the extraction of vanadium, *Int. J. Miner. Process.*, 95(2010), No. 1-4, p. 62.
- [10] M.Y. Wang, L.S. Xiao, Q.G. Li, X.W. Wang, and X.Y. Xiang, Leaching of vanadium from stone coal with sulfuric acid, *Rare Met.*, 28(2009), No. 1, p. 1.
- [11] B. Zhang, Z.G. Gao, H.Z. Liu, W. Wang, and Y.H. Cao, Direct acid leaching of vanadium from stone coal, *High Temp. Mater. Process.*, 36(2017), No. 9, p. 877.
- [12] X.Y. Zhang, K. Yang, X.D. Tian, and W.Q. Qin, Vanadium leaching from carbonaceous shale using fluosilicic acid, *Int. J. Miner. Process.*, 100(2011), No. 3-4, p. 184.
- [13] A.M. Elmahdy, M. Farahat, and T. Hirajima, Comparison between the effect of microwave irradiation and conventional heat treatments on the magnetic properties of chalcopyrite and pyrite, *Adv. Powder Technol.*, 27(2016), No. 6, p. 2424.
- [14] Z. Moravvej, A. Mohebbi, and S. Daneshpajouh, The microwave irradiation effect on copper leaching from sulfide/oxide ores, *Mater. Manuf. Process.*, 33(2018), No. 1, p. 1.
- [15] T. Le, X.T. Li, A.V. Ravindra, Q. Wang, J.H. Peng, and S.H. Ju, Leaching behavior of contaminant metals from spent FCC catalyst under microwave irradiation, *Mater. Res. Express*,

- 6(2018), No. 3, art. No. 035509.
- [16] L. Guo, J.R. Lan, Y.G. Du, T.C. Zhang, and D.Y. Du, Microwave-enhanced selective leaching of arsenic from copper smelting flue dusts, *J. Hazard. Mater.*, 386(2020), art. No. 121964.
- [17] T. Wen, Y.L. Zhao, Q.H. Xiao, *et al.*, Effect of microwave-assisted heating on chalcopyrite leaching of kinetics, interface temperature and surface energy, *Results Phys.*, 7(2017), p. 2594.
- [18] L.Y. Zhang, J.M. Mo, X.H. Li, L.P. Pan, and G.T. Wei, Leaching reaction and kinetics of zinc from indium-bearing zinc ferrite under microwave heating, *Russ. J. Non-Ferrous Met.*, 57(2016), No. 4, p. 301.
- [19] J.P. Wang, Y.M. Zhang, J. Huang, and T. Liu, Synergistic effect of microwave irradiation and  $\text{CaF}_2$  on vanadium leaching, *Int. J. Miner. Metall. Mater.*, 24(2017), No. 2, p. 156.
- [20] J.P. Wang, Y.M. Zhang, J. Huang, and T. Liu, Efficient microwave irradiation-assisted hydrothermal synthesis of ammonium vanadate flake, *Cryst. Res. Technol.*, 52(2017), No. 12, art. No. 1700104.
- [21] X. Qiao and X.Y. Xie, The effect of electric field intensification at interparticle contacts in microwave sintering, *Sci. Reports*, 6(2016), art. No. 32163.
- [22] T. Ebadzadeh, Effect of mechanical activation and microwave heating on synthesis and sintering of nano-structured mullite, *J. Alloys Compd.*, 489(2010), No. 1, p. 125.
- [23] X.F. Zhang, F.G. Liu, X.X. Xue, and T. Jiang, Effects of microwave and conventional blank roasting on oxidation behavior, microstructure and surface morphology of vanadium slag with high chromium content, *J. Alloys Compd.*, 686(2016), p. 356.
- [24] A.J. Teng and X.X. Xue, A novel roasting process to extract vanadium and chromium from high chromium vanadium slag using a  $\text{NaOH}\text{--}\text{NaNO}_3$  binary system, *J. Hazard. Mater.*, 379(2019), art. No. 120805.
- [25] H.Y. Gao, T. Jiang, M. Zhou, J. Wen, X. Li, Y. Wang, and X.X. Xue, Effect of microwave irradiation and conventional calcification roasting with calcium hydroxide on the extraction of vanadium and chromium from high-chromium vanadium slag, *Miner. Eng.*, 145(2020), art. No. 106056.
- [26] Y.Z. Yuan, Y.M. Zhang, T. Liu, T.J. Chen, and J. Huang, Comparison of microwave and conventional blank roasting and of their effects on vanadium oxidation in stone coal, *J. Microwave Power Electromagn. Energy*, 50(2016), No. 2, p. 81.
- [27] Y.Z. Yuan, Y.M. Zhang, T. Liu, and T.J. Chen, Comparison of the mechanisms of microwave roasting and conventional roasting and of their effects on vanadium extraction from stone coal, *Int. J. Miner. Metall. Mater.*, 22(2015), No. 5, p. 476.
- [28] E.A. Olevsky, A.L. Maximenko, and E.G. Grigoryev, Ponderomotive effects during contact formation in microwave sintering, *Modelling Simul. Mater. Sci. Eng.*, 21(2013), No. 5, art. No. 055022.
- [29] K.I. Rybakov, E.A. Olevsky, and V.E. Semenov, The microwave ponderomotive effect on ceramic sintering, *Scripta Mater.*, 66(2012), No. 12, p. 1049.
- [30] S.A. Freeman, J.H. Booske, and R.F. Cooper, Microwave field enhancement of charge transport in sodium chloride, *Phys. Rev. Lett.*, 74(1995), No. 11, p. 2042.
- [31] D. Demirskyi, D. Agrawal, and A. Ragulya, Neck growth kinetics during microwave sintering of copper, *Scripta Mater.*, 62(2010), No. 8, p. 552.
- [32] X. Wang, D.J. Yang, C. Srinivasakannan, J.H. Peng, X.H. Duan, and S.H. Ju, A comparison of the conventional and ultrasound-augmented leaching of zinc residue using sulphuric acid, *Arab. J. Sci. Eng.*, 39(2014), No. 1, p. 163.
- [33] J.Y. Xiang, Q.Y. Huang, X.W. Lv, and C.G. Bai, Extraction of vanadium from converter slag by two-step sulfuric acid leaching process, *J. Clean. Prod.*, 170(2018), p. 1089.
- [34] J.Y. Xiang, Q.Y. Huang, X.W. Lv, and C.G. Bai, Effect of mechanical activation treatment on the recovery of vanadium from converter slag, *Metall. Mater. Trans. B*, 48(2017), No. 5, p. 2759.
- [35] Q.W. Yang, Z.M. Xie, H. Peng, Z.H. Liu, and C.Y. Tao, Leaching of vanadium and chromium from converter vanadium slag intensified with surface wettability, *J. Central South Univ.*, 25(2018), No. 6, p. 1317.
- [36] J.P. Wang, Y.M. Zhang, J. Huang, and T. Liu, Kinetic and mechanism study of vanadium acid leaching from black shale using microwave heating method, *JOM*, 70(2018), No. 6, p. 1031.
- [37] F. Wang, Y.M. Zhang, J. Huang, *et al.*, Mechanisms of acid-leaching reagent calcium fluoride in the extracting vanadium processes from stone coal, *Rare Met.*, 32(2013), No. 1, p. 57.
- [38] J. Sun, W.L. Wang, Q.Y. Yue, *et al.*, Review on microwave-metal discharges and their applications in energy and industrial processes, *Appl. Energy*, 175(2016), p. 141.
- [39] J.Y. Zhu, L.P. Yi, Z.Z. Yang, and M. Duan, Three-dimensional numerical simulation on the thermal response of oil shale subjected to microwave heating, *Chem. Eng. J.*, 407(2021), art. No. 127197.